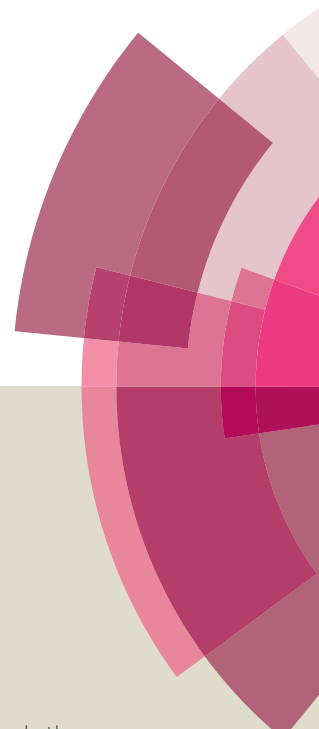


Catalysis Science & Technology

Accepted Manuscript



This article can be cited before page numbers have been issued, to do this please use: Y. Kuwahara, Y. Yoshimura and H. Yamashita, *Catal. Sci. Technol.*, 2015, DOI: 10.1039/C5CY01308A.



This is an *Accepted Manuscript*, which has been through the Royal Society of Chemistry peer review process and has been accepted for publication.

Accepted Manuscripts are published online shortly after acceptance, before technical editing, formatting and proof reading. Using this free service, authors can make their results available to the community, in citable form, before we publish the edited article. We will replace this *Accepted Manuscript* with the edited and formatted *Advance Article* as soon as it is available.

You can find more information about *Accepted Manuscripts* in the [Information for Authors](#).

Please note that technical editing may introduce minor changes to the text and/or graphics, which may alter content. The journal's standard [Terms & Conditions](#) and the [Ethical guidelines](#) still apply. In no event shall the Royal Society of Chemistry be held responsible for any errors or omissions in this *Accepted Manuscript* or any consequences arising from the use of any information it contains.

In situ-created Mn(III) complex active for liquid-phase oxidation of alkylaromatics to aromatic ketones with molecular oxygen

Yasutaka Kuwahara,^{a,b} Yukihiro Yoshimura^a and Hiromi Yamashita^{a,b*}

Received 00th January 20xx,
Accepted 00th January 20xx

DOI: 10.1039/x0xx00000x

www.rsc.org/

Liquid-phase oxidation of alkylaromatics with molecular O₂ over manganese hydroxide catalysts supported on various oxides was examined. Reaction kinetics in the ethylbenzene oxidation with O₂ indicated some configurational/electronic alterations of Mn species during the induction period of the reaction due to the interaction with benzoic acid. Characterization by means of FT-IR and XAFS revealed that Mn(OH)_x species was easily transformed into monomeric Mn(III) species coordinated with PhCOO⁻ ligand and anchored on the oxide support surface during the initial induction period of the reaction, which was the real active species. Among the catalyst examined, the *in situ*-created Mn species supported on γ-Al₂O₃ particularly exhibited a superior catalytic activity with good ketone selectivity compared to the other supported Mn catalysts. Moreover, leaching and agglomeration of the active Mn(III) species were scarcely observed, and the recovered catalyst was reusable without significant loss of activity in the presence of benzoic acid ligand. Such *in situ*-created Mn(III) species offer a simple, reusable and efficient oxidation system for alkylaromatics, such as ethylbenzene and diphenylmethane, of which activity is greater than that of its unsupported counterpart.

1. Introduction

Aromatic ketones are important chemical intermediates in the pharmaceutical, agrochemical, fragrance, and dye industries.¹ Aromatic ketones can be produced by Friedel–Crafts acylation of aromatic compounds catalyzed by a stoichiometric amount of homogeneous Lewis acids (e.g., AlCl₃, BF₃, FeCl₃ etc.) or strong protonic acids (e.g., H₂SO₄, HF), which leads to the formation of a large volume of toxic and corrosive wastes.² An alternative pathway to produce aromatic ketones is direct oxidation of alkylaromatics using stoichiometric quantities of oxidizing agent (e.g., KMnO₄,³ TBHP,⁴⁻¹³ and H₂O₂¹⁴). Current route to produce aromatic ketones in industry employs direct oxidation of alkylaromatics with molecular oxygen, a more environmentally-friendly oxidant, using cobalt acetate as a catalyst in acetic acid media.¹⁵ However, these oxidation processes generate large volume of waste and always suffer from separation problems of catalysts. From environmental and practical standpoints, it is necessary to develop recyclable heterogeneous catalyst that efficiently works for the oxidation of alkylaromatics using O₂ as an oxidant under liquid-phase condition, more preferably under solvent-free condition.

Transition metal (e.g., Cr, Mn, Co)-based catalysts have recently been reported to act as heterogeneous catalysts for the oxidation of alkylaromatics with molecular O₂.¹⁶⁻¹⁸ Among

those, Mn-based catalysts have been proven to be superior compared to the other transition metal-based catalysts due to the diverse oxidation states that are suitable to drive the demanding oxidation reactions as well as low toxicity and ready availability.¹⁹ Earlier reports utilized Mn salts (e.g. manganese stearate and manganese acetate) for the oxidation of ethylbenzene to acetophenone with O₂. However, the separation of reactants and catalysts from the reaction mixture is difficult, and the reaction starts after a lengthy induction period.^{20,21} Mn complexes (e.g. Mn porphyrin) have also been used as the catalysts, but the problem associated with reusability limits their industrial application.²² Silica-supported manganese oxides have long been examined for aerobic oxidation of ethylbenzene, but the reaction requires either high temperatures (~350 °C, in vapour-phase condition) or high pressures (ca. 10 atm, in liquid-phase condition).^{23,24} Choudhary et al. recently reported that MgAl hydrotalcite-supported Mn catalyst acts as an effective heterogeneous catalyst for the oxidation of several alkylaromatics with atmospheric pressure of O₂ under solvent-free conditions.^{25,26} Indeed, the predominant focus in this oxidation system to date has been on altering the type of support materials and observing the reaction kinetics. However, local structures of the Mn species which is truly active for this reaction have never been investigated.^{27,28}

In this study, liquid-phase oxidation of alkylaromatics with molecular O₂ using simple supported manganese catalysts was examined and the local structure of the real active Mn species was investigated. Characterizations by means of fourier transform infrared spectroscopy (FT-IR) and X-ray absorption fine structure (XAFS) revealed the initial Mn species

^a Division of Materials and Manufacturing Science, Graduate School of Engineering, Osaka University, 2-1 Yamada-oka, Suita, Osaka 565-0871

^b Unit of Elements Strategy Initiative for Catalysts & Batteries (ESICB), Kyoto University, Katsura, Kyoto 615-8520

† Electronic Supplementary Information (ESI) available: XRD, reaction kinetics and XAFS analysis data of the catalysts. See DOI: 10.1039/x0xx00000x

transformed into a monomeric active Mn(III) species ligated by PhCOO^- and anchored on oxide support surface, which exhibited a superior catalytic activity in the oxidation of alkylaromatics with molecular O_2 compared to the unsupported counterpart. We also examined the effect of oxide support type and the scope of substrate as well as the recyclability of the catalyst.

2. Experimental

2.1. Materials

All commercially available chemical reagents for material synthesis and catalytic tests were purchased from Nacal Tesque, Inc. and used without further purification. A variety of metal oxides were used as supports for $\text{Mn}(\text{OH})_x$ catalyst; $\gamma\text{-Al}_2\text{O}_3$ (JRC-ALO-4, $S_{\text{BET}} = 210 \text{ m}^2/\text{g}$) was supplied from Catalysis Society of Japan. SiO_2 ($S_{\text{BET}} = 280 \text{ m}^2/\text{g}$) and MgO ($S_{\text{BET}} = 45 \text{ m}^2/\text{g}$) were purchased from Wako Pure Chemical Ind., Ltd. Anatase TiO_2 (ST-01, $S_{\text{BET}} = 339 \text{ m}^2/\text{g}$) was supplied from Ishihara Sangyo Co., Ltd.

2.2. Catalyst preparation

$\text{Mn}(\text{OH})_x$ catalysts supported on a variety of metal oxides were prepared by the conventional precipitation method.^{29,30} Typically, oxide support (1.0 g) pretreated at 550 °C for 3 h in air was mixed with 30 mL of an aqueous solution of $\text{MnCl}_2 \cdot 4\text{H}_2\text{O}$ (6 mM) for 15 min with magnetic stirring. The pH of the solution was adjusted to 12 by adding an aqueous NaOH solution (1.0 M). After stirring for 24 h at room temperature, the obtained solid was isolated by filtration, washed with a copious amount of deionized water, and dried at room temperature in vacuo, yielding supported $\text{Mn}(\text{OH})_x$ catalyst as a brown powder. Mn content was adjusted to be 1.0 wt.%. Pure $\text{Mn}(\text{OH})_3$ was synthesized with a similar procedure except for the addition of oxide support.

2.3. Characterization

Powder XRD patterns were recorded on a Rigaku Ultima IV diffractometer with $\text{CuK}\alpha$ radiation ($\lambda = 1.54056 \text{ \AA}$, 40 kV–40 mA). BET surface area measurements were performed using BELSORP-max system (BEL Japan, Inc.) at -196 °C. The samples were degassed at 200 °C under vacuum for 3 h prior to the measurements to vaporize physisorbed water. The surface area was calculated by the BET (Brunauer–Emmett–Teller) method by using adsorption data ranging from $P/P_0 = 0.05$ to 0.30. Mn loadings were determined by inductively coupled plasma atomic emission spectrometry (ICP-AES) using a Nippon Jarrell-Ash ICAP-575 Mark II instrument. Infrared spectra were recorded on a JASCO FTIR-6300 instrument in the spectral range 2000–400 cm^{-1} under vacuum with a resolution of 4 cm^{-1} using samples diluted with KBr. Mn K-edge XAFS spectra were recorded in fluorescence mode at room temperature at BL01B1 facility with an attached Si(111) monochromator at SPring-8 (JASRI), Hyogo, Japan. All EXAFS data were normalized by fitting the background absorption coefficient, around the energy region higher than that of the

edge position of about 35–50 eV. The EXAFS data were examined by using Rigaku REX2000 software, by which Fourier transformation of k^3 -weighted normalized EXAFS data (FT-EXAFS) was performed over the range $3.0 < k(\text{\AA}^{-1}) < 11.0$ to obtain the radial structure function (RDF). For the curve-fitting analysis, the empirical phase shift and amplitude functions for Mn–O and Mn–Mn were extracted from the data for Mn_2O_3 assuming an octahedral coordination geometry.

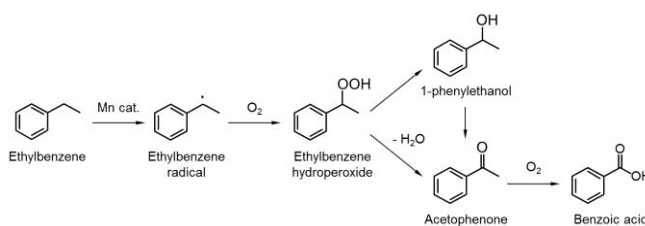
2.4. Typical procedures for catalytic reactions

To a glass reactor equipped with a water-cooled condenser and connected to an O_2 gas cylinder through a Teflon® tube were added alkylaromatics (40 mmol) and catalyst (Mn 0.03 mmol). The reaction mixture was stirred vigorously at 135 °C under a flow of O_2 (5 mL/min) with magnetic stirring. After allotted time intervals, the reaction mixture was withdrawn, filtered and analyzed by a gas chromatograph (Shimadzu GC-14B) with a flame ionization detector equipped with a capillary column (Zebron ZB-FFAP; 0.32 mm \times 50 m; phenomenex®). Yields of products were determined by using biphenyl as an internal standard. For recycle test of catalyst, the spent catalyst was recovered by filtration, washed with acetone, dried under vacuum, and then subjected to next catalytic run.

3. Results and discussion

3.1. Oxidation of ethylbenzene

In the preliminary study, several manganese oxide/hydroxide catalysts were tested in the liquid-phase oxidation of ethylbenzene with molecular O_2 at 135 °C under solvent-free conditions. In this reaction, acetophenone was produced as a major product, and 1-phenylethanol and benzoic acid were detected as major byproducts together with trace of ethylbenzene hydroperoxide. Generally, in the ethylbenzene oxidation with O_2 over Mn-based catalyst, acetophenone is known to be produced from ethylbenzene hydroperoxide *via* ethylbenzene radical as an intermediate, and benzoic acid is produced by the successive oxidation of acetophenone (Scheme 1).^{20,21,25,26} When 0.075 mol% Mn was used, $\text{Mn}(\text{III})(\text{OH})_3$ and $\text{Mn}(\text{III})_2\text{O}_3$ afforded higher conversions (21–22%) with acetophenone selectivities of 63–68% after 9 h of reaction compared to the other manganese oxides such as $\text{Mn}(\text{II})\text{O}$ and $\text{Mn}(\text{IV})\text{O}_2$ (conversions < 12%), suggesting that trivalent Mn species acts as an active catalyst for this reaction.²⁰ Especially, $\text{Mn}(\text{OH})_3$ afforded the fastest reaction rate compared to the others, demonstrating that hydroxide form of Mn is the promising precursor for this reaction.



Scheme 1 Reaction pathway in the oxidation of ethylbenzene with molecular O_2 .

Next, a fixation of manganese hydroxides to oxide supports was examined in order to improve the stability and recyclability. $\text{Mn}(\text{OH})_x$ catalysts supported on a variety of metal oxides were prepared by the conventional precipitation method in alkaline aqueous solution. Elemental analysis confirmed that the Mn content was ca. 1.0 wt.% in all cases. The X-ray diffraction (XRD) patterns of supported $\text{Mn}(\text{OH})_x$ catalysts were identical to those of the parent supports and no diffraction peaks assignable to either $\text{Mn}(\text{OH})_x$ or manganese oxides were observed in all cases (see Fig. S1 in ESI[†]), suggesting the formation of small $\text{Mn}(\text{OH})_x$ particles with uniform dispersion.

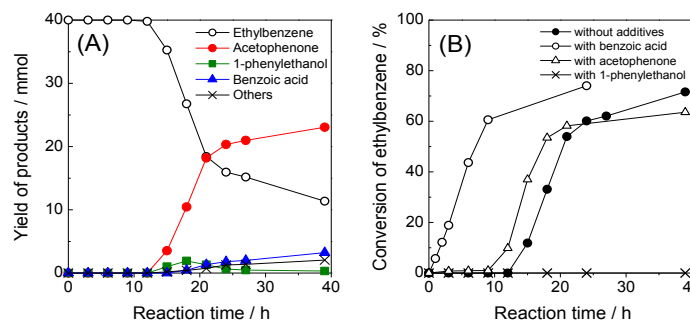


Fig. 1 (A) Reaction kinetics in the liquid-phase oxidation of ethylbenzene with molecular O_2 at 135 °C over $\text{Mn}(\text{OH})_x/\gamma\text{-Al}_2\text{O}_3$ catalyst. (B) Comparison of conversions of ethylbenzene over $\text{Mn}(\text{OH})_x/\gamma\text{-Al}_2\text{O}_3$ with and without addition of 1 mol% of byproducts (acetophenone, 1-phenylethanol, and benzoic acid).

Fig. 1(A) shows typical reaction kinetics in the liquid-phase oxidation of ethylbenzene with molecular O_2 at 135 °C over $\text{Mn}(\text{OH})_x/\gamma\text{-Al}_2\text{O}_3$ catalyst. When $\text{Mn}(\text{OH})_x/\gamma\text{-Al}_2\text{O}_3$ was used alone, 62% yield of acetophenone was attained after 39 h of reaction together with the formation of small quantities of 1-phenylethanol and benzoic acid, but a lengthy induction period of 12 h was observed before the reaction was initiated. This result agrees well with the previous report by Bukharkina et al, who speculated based on reaction kinetics data that there is some changes of Mn species during the induction period due to the interaction with the products (exact structure of active Mn species has not been proposed).²⁰ Based on the hypothesis that specific products provide some productive effects on Mn species, the reaction was performed in the presence of the products (acetophenone, 1-phenylethanol or benzoic acid). As shown in Fig. 1(B), addition of small amount (1 mol%) of benzoic acid in the reaction system drastically reduced the induction period, while addition of 1 mol% of acetophenone had little effect on the reaction kinetics, suggesting some configurational/electronic alterations of Mn species by the coordination with benzoic acid. On the other hand, addition of 1 mol% of 1-phenylethanol resulted in the complete loss of activity. This is attributed to the deactivation of Mn catalyst due to the coordination with 1-phenylethanol, which might prevent the productive configurational/electronic alterations of Mn species.²⁰ Similar reaction kinetics were also observed for the other supported $\text{Mn}(\text{OH})_x$ catalysts (see Fig. S2 in ESI[†]).

Table 1 summarizes the catalytic results in the liquid-phase oxidation of ethylbenzene using various supported $\text{Mn}(\text{OH})_x$

catalysts with the addition of 1 mol% of benzoic acid together with the BET surface area determined from N_2 adsorption isotherms and oxidation number (N_{oxi}) determined from XAFS analysis. Among the catalysts examined, $\text{Mn}(\text{OH})_x/\gamma\text{-Al}_2\text{O}_3$ exhibited the highest ethylbenzene conversion (61%) and acetophenone selectivity (84%) after 9 h at 135 °C (entry 3), which were higher than those for unsupported $\text{Mn}(\text{OH})_3$ (conv. = 40%, entry 1) and the physical mixture of $\text{Mn}(\text{OH})_3$ and $\gamma\text{-Al}_2\text{O}_3$ (conv. = 41%, entry 8), demonstrating that fixation of $\text{Mn}(\text{OH})_3$ on $\gamma\text{-Al}_2\text{O}_3$ support is an effective way to improve catalytic performances. $\text{Mn}(\text{OH})_x/\text{SiO}_2$ gave as high activities and selectivities (conv. = 58%, sel. = 79%, entry 5) as those of $\text{Mn}(\text{OH})_x/\gamma\text{-Al}_2\text{O}_3$; however, $\text{Mn}(\text{OH})_x/\text{SiO}_2$ caused a significant leaching of Mn species into the reaction solution during the reaction. $\text{Mn}(\text{OH})_x/\text{TiO}_2$ and $\text{Mn}(\text{OH})_x/\text{MgO}$ showed subpar activities compared to $\text{Mn}(\text{OH})_x/\gamma\text{-Al}_2\text{O}_3$ (conv. = 36–52%, entry 6,7), albeit the selectivity to acetophenone was scarcely changed. Ethylbenzene thermally-reacted with O_2 to afford oxidation products with 13.3% conversion in the presence of benzoic acid (entry 11), which was apparently lower than those for Mn-containing catalysts, elucidating that Mn is the dominant active species in this reaction. It is noteworthy that the addition of $\gamma\text{-Al}_2\text{O}_3$ gave a quite lower ethylbenzene conversion (1.8%, entry 10). This decrease in the ethylbenzene conversion is probably due to the ability of $\gamma\text{-Al}_2\text{O}_3$ to adsorb benzoic acid, leaving the possibility that benzoic acid is acting also as an initiator to produce hydrocarbon radical species in this reaction.

Table 1 Liquid-phase oxidation of ethylbenzene with molecular O_2 in the presence of benzoic acid using various $\text{Mn}(\text{OH})_x$ catalysts.^a

Entry	Catalyst	N_{oxi}^b	S_{BET}^c (m ² /g)	Conv. (%)	S_{ketone} (%)
1	$\text{Mn}(\text{OH})_3$	2.8	-	40	80
2 ^d	$\text{Mn}(\text{OH})_3$	2.8	-	21	63
3	$\text{Mn}(\text{OH})_x/\gamma\text{-Al}_2\text{O}_3$	3.6	182	61	84
4 ^d	$\text{Mn}(\text{OH})_x/\gamma\text{-Al}_2\text{O}_3$	3.6	182	0	-
5	$\text{Mn}(\text{OH})_x/\text{SiO}_2$	3.1	167	58	79
6	$\text{Mn}(\text{OH})_x/\text{TiO}_2$	3.4	50	36	74
7	$\text{Mn}(\text{OH})_x/\text{MgO}$	4.8	72	52	81
8	$\text{Mn}(\text{OH})_3 + \gamma\text{-Al}_2\text{O}_3$	2.8	-	41	66
9	$\text{Mn}(\text{PhCOO})_2^+$	3.0	-	56	79
10	$\gamma\text{-Al}_2\text{O}_3$	-	210	1.8	81
11	none	-	-	13.3	64

^a Reaction conditions: catalyst (Mn 0.03 mmol), ethylbenzene (40 mmol), benzoic acid (0.4 mmol), O_2 flow (5 mL/min), 135 °C, 9 h. ^b Oxidation number of Mn determined from XANES spectra. ^c Surface area determined by BET method. ^d Without addition of benzoic acid.

As summarized in Table 1, there is no link between the activities and surface areas of the supports, indicating that surface area and the associated accessibility of substrate is not a dominating factor in this reaction. However, a noticeable correlation was observed between the lengths of the induction

periods and the N_{oxi} of the catalysts: although $\text{Mn}(\text{OH})_x/\gamma\text{-Al}_2\text{O}_3$ with N_{oxi} of 3.6 exhibited a lengthy induction period of 12 h, $\text{Mn}(\text{OH})_x/\text{TiO}_2$ with N_{oxi} of 3.4 exhibited shorter induction period of about 3 h and $\text{Mn}(\text{OH})_x/\text{SiO}_2$ with N_{oxi} of 3.1 exhibited no induction period in the absence of benzoic acid (see Fig. S2 in ESI[†]). These results demonstrate that the type of support offers different oxidation state for $\text{Mn}(\text{OH})_x$ species, and $\text{Mn}(\text{OH})_x$ species with N_{oxi} close to 3+ easily undergoes configurational/electronic changes to form real active Mn species *via* a coordination with benzoic acid.

3.2. Investigation of active Mn species

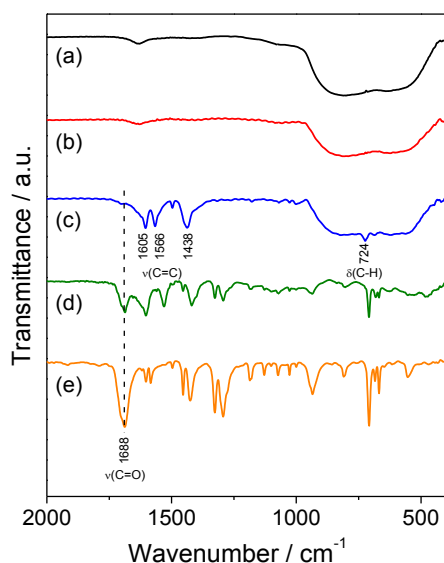


Fig. 2 FT-IR spectra of (a) $\gamma\text{-Al}_2\text{O}_3$, (b) fresh $\text{Mn}(\text{OH})_x/\gamma\text{-Al}_2\text{O}_3$, (c) used $\text{Mn}(\text{OH})_x/\gamma\text{-Al}_2\text{O}_3$, (d) $\text{Mn}(\text{PhCOO})_2^+$ complex, and (e) benzoic acid.

In order to investigate the chemical environment of active Mn species created during the reaction, $\text{Mn}(\text{OH})_x/\gamma\text{-Al}_2\text{O}_3$ catalyst before and after the reaction was characterized by FT-IR and XAFS measurements. In the IR spectrum of used $\text{Mn}(\text{OH})_x/\gamma\text{-Al}_2\text{O}_3$, distinct absorption bands were newly observed at 1605, 1566, 1438, and 724 cm^{-1} (Fig. 2). The bands at 1605, 1566, and 1438 cm^{-1} are all assignable to stretching vibrations of aromatic ring, and the band at 724 cm^{-1} is ascribed to out-of-plane bending vibration of C–H bond.³¹ A shoulder peak assignable to the stretching vibration of C=O bond typically seen for benzoic acid was observed at around 1690 cm^{-1} , indicating the presence of benzoic acid adsorbed on the catalyst surface. Intensity of this band was significantly weakened compared to those of benzoic acid and Mn–benzoic acid complex ($\text{Mn}(\text{PhCOO})_2^+$). Considering the fact that the proportion of Mn atoms present on the $\text{Mn}(\text{OH})_x/\gamma\text{-Al}_2\text{O}_3$ surface is quite small, most of the benzoic acid is chemisorbed on $\gamma\text{-Al}_2\text{O}_3$ surface in the form of carboxylate species, although the possibility of adsorption of other aromatic compounds such as 1-phenylethanol cannot completely be excluded from this result.

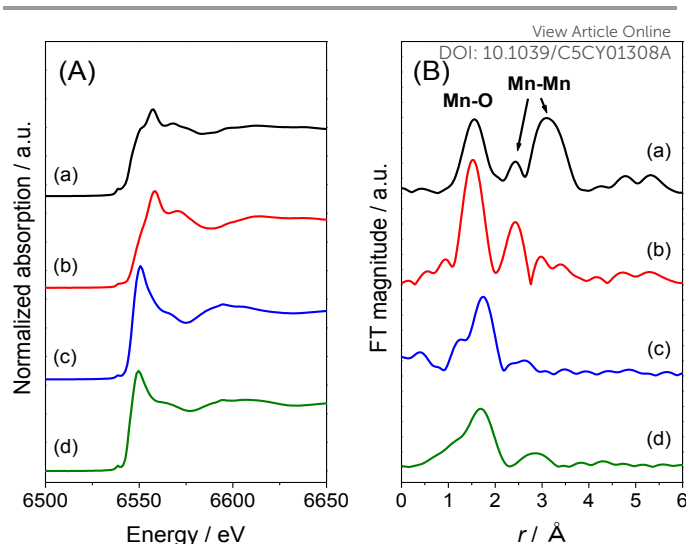


Fig. 3 (A) Mn K-edge XANES spectra and (B) Mn K-edge radial distribution functions of (a) $\text{Mn}(\text{OH})_3$, (b) fresh $\text{Mn}(\text{OH})_x/\gamma\text{-Al}_2\text{O}_3$, (c) used $\text{Mn}(\text{OH})_x/\gamma\text{-Al}_2\text{O}_3$, and (d) $\text{Mn}(\text{PhCOO})_2^+$ complex.

The shape and edge position of Mn K-edge X-ray absorption near edge structure (XANES) spectrum of used $\text{Mn}(\text{OH})_x/\gamma\text{-Al}_2\text{O}_3$ were similar to those of $\text{Mn}(\text{PhCOO})_2^+$ complex in square planar coordination but differed from those of $\text{Mn}(\text{OH})_3$ and fresh catalyst with a typical octahedral coordination geometry (Fig. 3(A)).^{32,33} The oxidation number (N_{oxi}) of reference Mn compounds (Mn foil, MnO, Mn_2O_3 , MnO_2 , and KMnO_4) plotted against energy shift of the edge (based on the edge of Mn foil) provides a linear correlation as shown in Fig. 4 (for XANES spectra and their first derivatives, see Fig. S3 in ESI[†]).^{30,32,33} By the linear interpolation method, the N_{oxi} of $\text{Mn}(\text{OH})_x/\gamma\text{-Al}_2\text{O}_3$ catalyst before and after the reaction was determined to be 3.6 and 3.1, respectively. This indicates that the Mn in the used catalyst is dominantly present in the 3+ oxidation state in square planar coordination geometry.

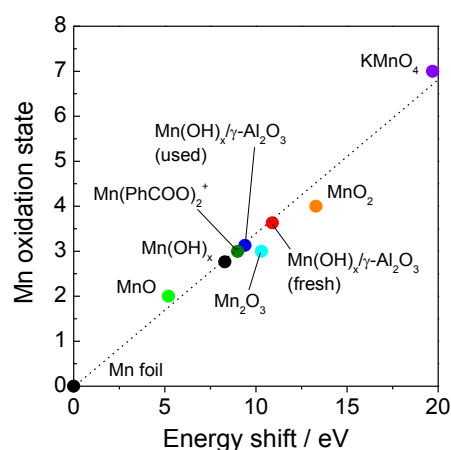


Fig. 4 Correlation between energy shift and oxidation state of Mn atoms in the experimental samples and reference Mn model compounds.

Table 2 Mn K-edge XANES and EXAFS curve-fitting parameters of Mn(OH)₃, fresh Mn(OH)_x/γ-Al₂O₃, used Mn(OH)_x/γ-Al₂O₃, and Mn(PhCOO)₂⁺.

Sample	E_0 (eV) ^b	N_{oxi} ^c	Shell	C.N. ^d	R^e (Å)	$\Delta\sigma^2$ (Å ²)
Mn(OH) ₃	6546.3	2.8	Mn–O	5.0	1.94	0.003
			Mn–Mn(1)	2.5	2.74	0.006
			Mn–Mn(2)	7.5	3.48	0.001
Mn(OH) _x /γ-Al ₂ O ₃ (fresh)	6548.9	3.6	Mn–O	5.6	1.94	0.001
			Mn–Mn	3.2	2.76	0.001
Mn(OH) _x /γ-Al ₂ O ₃ (used)	6547.4	3.1	Mn–O	3.8	2.14	0.004
			Mn–Mn	N.D.	N.D.	N.D.
Mn(PhCOO) ₂ ⁺	6547.0	3.0	Mn–O	4.0	2.26	0.001

^a k^3 -weighted EXAFS, $3.0 \leq k(\text{Å}^{-1}) \leq 13.0$. ^b Determined based on the first derivatives of XANES spectra. ^c Derived by the linear interpolation. ^d Average coordination number. ^e Average interatomic distance. N.D. = Not determined.

In the radial distribution functions (RDFs) of Mn(OH)₃ and fresh Mn(OH)_x/γ-Al₂O₃ (Fig. 3(B)), the peaks corresponding to Mn–O and Mn–Mn bonds were observed at around $r = 1.5$ and 2.4 Å (the phase shift uncorrected), respectively, due to the presence of oxygen-bridged contiguous Mn–Mn bonds.³⁴ After the catalytic use, the FT magnitude of the Mn–Mn shell signal almost disappeared, and the RDF showed a similar shape to that of Mn(PhCOO)₂⁺. In addition, the first Mn–O shell located at $r = 1.5$ Å apparently shifted toward a longer interatomic distance ($r = 1.7$ Å), which is close to that of Mn(PhCOO)₂⁺ ($r = 1.7$ Å). As shown in Table 2, it was confirmed by curve-fitting analysis that the coordination numbers (C.N.) of the Mn–O shell of Mn(OH)_x/γ-Al₂O₃ decreased from 5.6 to 3.8, and the interatomic distance (R) between Mn and the neighboring oxygen atoms was changed from $R = 1.94$ Å to 2.14 Å after the catalytic use. These combined analyses indicates that the Mn(OH)_x species fixed on γ-Al₂O₃ transformed into monomeric Mn species with square planar geometry surrounded by PhCOO[−] ligand during the initial induction period of the reaction, which is the real active species for this reaction.³⁵ The most plausible Mn structures created during the reaction is illustrated in Fig. 5. Since the leaching of Mn during the reaction was negligible (will be discussed later), most of Mn species is probably existing as bidentate Mn(III) species anchored on γ-Al₂O₃ surface *via* two oxygen atoms and coordinated with one PhCOO[−] ligand, otherwise, creating a Mn(III)(PhCOO)₂⁺ complex, which might be adsorbed on support surface through electrostatic interaction. In fact, the oxidation reaction of ethylbenzene using Mn(III)(PhCOO)₂⁺ complex as a catalyst afforded 56% ethylbenzene conversion with 79% acetophenone selectivity (Table 1, entry 9), which was almost similar to those obtained over supported Mn(OH)_x catalysts. This result strongly supports the above idea. Considering the fact that γ-Al₂O₃ is the most suitable support in this reaction, an appropriate surface acid-base property of γ-Al₂O₃ is likely playing an important role to create such a stable active species.³⁵

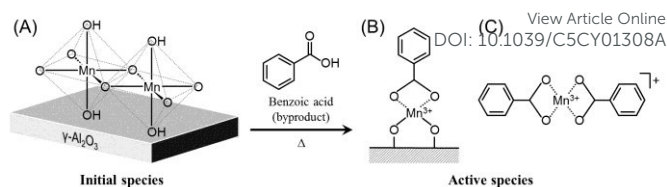


Fig. 5. Schematic illustration of transformation of (A) Mn(OH)_x species supported on γ-Al₂O₃ into (B,C) plausible structure of in situ-created active Mn species during the reaction.

3.3. Catalyst recyclability and the scope of substrate

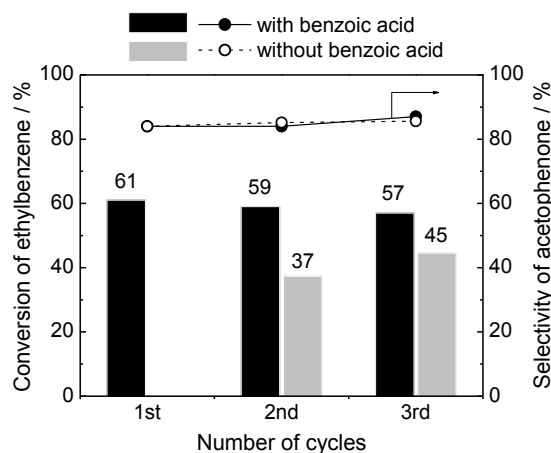
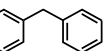
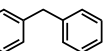
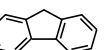
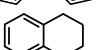
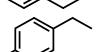


Fig. 6 Recyclability test of Mn(OH)_x/γ-Al₂O₃ catalyst with and without addition of benzoic acid into the initial reaction mixture. Reaction conditions: catalyst (Mn 0.03 mmol), ethylbenzene (40 mmol), benzoic acid (0.4 mmol), O₂ flow (5 mL/min), 135 °C, 9 h.

To evaluate the recyclability and stability of the catalysts, oxidation of ethylbenzene with O₂ under solvent-free condition was performed over 3 successive cycles using Mn(OH)_x/γ-Al₂O₃ catalyst with and without addition of benzoic acid as a ligand into the reaction mixture (Fig. 6). After each catalytic run, the catalyst was recovered from the reaction mixture by filtration, washed with acetone, dried under vacuum, and then subjected to next catalytic run. With the addition of benzoic acid to the starting reaction mixture in each run, the Mn(OH)_x/γ-Al₂O₃ catalyst showed as similar reaction rate as that of 1st catalytic run, and was repeatedly reusable at least 3 cycles with retaining most of its catalytic performance. Moreover, leaching of Mn species into the reaction mixture during the reaction was negligible (Mn content: 0.99 → 0.94 wt.%), and the recovered catalyst maintained its original Mn structure and oxidation state as confirmed by XAFS (Fig. S4 in ESI[†]), demonstrating a promising recyclability. On the other hand, a considerable loss of catalytic activity was observed without the addition of benzoic acid in each catalytic run, although the selectivity to acetophenone remained unchanged. This might be attributed to the competitive coordination of 1-phenylethanol to the Mn species which causes the deactivation of the catalyst.

Table 3. Scope of substrates for the liquid-phase oxidation of alkylaromatics to aromatic ketones over Mn(OH)_x/γ-Al₂O₃ catalyst.

Entry	Substrate	t (h)	Conv. (%)	Selectivity (%)		
				Ketone	Alcohol	Others
1 ^a		9	61	84	7	9
2 ^a		24	74	86	3	11
3 ^{a,c}		24	52	70	10	20
4 ^a		9	26	86	12	2
5 ^a		24	46	93	4	3
6 ^b		9	29	88	10	2
7 ^b		9	57	42	7	51
8 ^b		9	63	39	3	58

^a Reaction conditions: catalyst (Mn 0.03 mmol), substrate (40 mmol), benzoic acid (0.4 mmol), O₂ flow (5 mL/min), 135 °C. ^b Reaction conditions: catalyst (Mn 0.03 mmol), substrate (5 mmol), solvent (*m*-dichlorobenzene, 5 mL), benzoic acid (0.4 mmol), O₂ flow (5 mL/min), 135 °C. ^c Air flow (5 mL/min) instead of O₂ flow.

Table 3 shows the scope of substrates for the liquid-phase oxidation of alkylaromatics with molecular O₂ using Mn(OH)_x/γ-Al₂O₃ catalyst together with 1 mol% of benzoic acid to form the real active Mn species. 74% conversion and 86% ketone selectivity was achieved after 24 h of reaction in the oxidation of ethylbenzene (entry 2). Furthermore, the reaction proceeded even under the flow of air, affording 52% ethylbenzene conversion and 70% acetophenone selectivity after 24 h of reaction (entry 3). Diphenylmethane and fluorene possessing active methylene groups afforded the corresponding ketones with 26–29% conversions and good ketone selectivities (86–88%) after 9 h of reaction (entry 4,6). However, tetralin and 4-ethyltoluene gave poor ketone selectivities (39–42%) under the same reaction conditions (entry 7,8). Comparative studies using a radical scavenger (hydroquinone) verified that the reaction involves radical alkylaromatics, which are generated due to the abstraction of hydrogen atoms from the alkylaromatics at benzylic positions by the Mn species and then readily trapped by dioxygen to form oxygenated compounds (Scheme 1).^{20,21,25,26} GC-MS analysis of the reaction solutions of tetralin and 4-ethyltoluene confirmed the formation of multiple oxygenated hydrocarbon compounds including polymerized species and their oxygenated derivatives, whereas only a few oxygenated compounds were detected in the reaction solutions of diphenylmethane and fluorene. The poor ketone selectivities for tetralin and 4-ethyltoluene are due to the formation of multiple hydrocarbon radical species and the sequential non-selective radical addition reactions.

Conclusions

In summary, we have found that supported manganese hydroxides acted as active heterogeneous catalysts for liquid-phase oxidation of alkylaromatics using molecular O₂ as a sole oxidant. This was due to the creation of monomeric Mn(III) species coordinated with PhCOO⁻ ligand and anchored on oxide support surface during the reaction, which was confirmed by spectroscopic analyses. In particular, the *in situ*-created Mn species supported on γ-Al₂O₃ was demonstrated to show a superior catalytic activity with good ketone selectivity compared to the other supported Mn catalysts. Although the scope of substrate is limited, such *in situ*-created Mn species offer a simple, reusable and efficient oxidation system for some important alkylaromatics, such as ethylbenzene and diphenylmethane, of which activity is greater than that of its unsupported counterpart.

Acknowledgements

This study was financially supported by the Grant-in-Aid from Frontier Research Base for Global Young Researchers, Osaka University and the Grant-in-Aid for Scientific Research (KAKENHI) from the Japan Society for the Promotion of Science (JSPS) (No. 15K18270). A part of this work was also performed under a management of "Elements Strategy Initiative for Catalysts & Batteries (ESICB)" supported by MEXT. The synchrotron radiation experiments were performed at the BL01B1 beam line in SPring-8 with the approval of JASRI (No. 2014B1041).

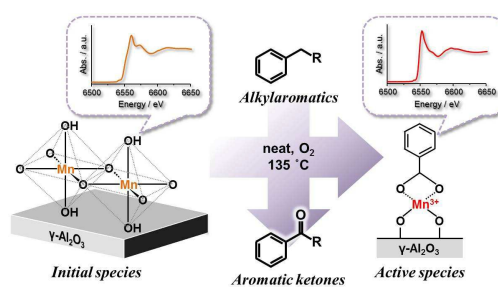
Notes and references

- H. J. Sanders, H. F. Keag and H. S. McCullough, *Ind. Eng. Chem.*, 1953, **45**, 2-14.
- G. A. Olah, in: *Friedel-Crafts and Related Reactions*, vols. I-IV, Wiley-Interscience, New York, 1963-1964.
- C. F. Cullis and J. W. Ladbury, *J. Chem. Soc.*, 1955, 2850-2854.
- S. Vetrivel and A. Pandurangan, *J. Mol. Catal. A*, 2004, **217**, 165-174.
- G. S. Kumar, M. Palanichamy, M. Hartmann and V. Murugesan, *Catal. Commun.*, 2007, **8**, 493-497.
- K. George and S. Sugunan, *Catal. Commun.*, 2008, **9**, 2149-2153.
- K. M. Parida and S. S. Dash, *J. Mol. Catal. A*, 2009, **306**, 54-61.
- M. Ghiaci, F. Molaie, M. E. Sedaghat and N. Dorostkar, *Catal. Commun.*, 2010, **11**, 694-699.
- M. Arshadi and M. Ghiaci, *Appl. Catal. A*, 2011, **399**, 75-86; M. Arshadi, M. Ghiaci, A. Rahmanian, H. Ghaziaskar and A. Gil, *Appl. Catal. B*, 2012, **119-120**, 81-90.
- D. Habibi and A. R. Faraji, *Appl. Surf. Sci.*, 2013, **276**, 487-496.
- P. Visuvamithiran, K. Shanthi, M. Palanichamy and V. Murugesan, *Catal. Sci. Technol.*, 2013, **3**, 2340-2348.
- X.-L. Yang, M.-H. Xie, C. Zou, Y. He, B. Chen, M. O'Keefe and C.-D. Wu, *J. Am. Chem. Soc.*, 2012, **134**, 10638-10645.
- P.-Q. Liao, X.-Y. Li, J. Bai, C.-T. He, D.-D. Zhou, W.-X. Zhang, J.-P. Zhang and X.-M. Chen, *Chem. Eur. J.*, 2014, **20**, 11303-11307.
- C. Lu, Z. Fu, Y. Liu, F. Liu, Y. Wu, J. Qin, X. He and D. Yin, *J. Mol. Catal. A*, 2010, **331**, 106-111.
- T. Maeda, A. K. Pee and D. Haa, JP Patent 07196573, 1995.
- I. C. Chisem, K. Martin, M. T. Shieh, J. Chisem, J. H. Clark, R. Jachuck, D. J. Macquarrie, J. Rafelt, C. Ramshaw and K. Scott, *Org. Proc. Res. Dev.*, 1997, **1**, 365-369.

- 17 J. H. Clark, A. P. Kybett, P. Landon, D. J. Macquarrie and K. Martin, *J. Chem. Soc., Chem. Commun.*, 1989, 1355-1356.
- 18 B. H. Monjezi, M. E. Yazdani, M. Mokfi and M. Ghiaci, *J. Mol. Catal. A*, 2014, **383-384**, 58-63.
- 19 Y. Kuwahara, K. Tsuji, T. Ohmichi, T. Kamegawa, K. Mori and H. Yamashita, *ChemSusChem*, 2012, **5**, 1523-1532.
- 20 T. V. Bukharkina, O. S. Grechishkina, N. G. Digurov and N. V. Krukovskaya, *Org. Proc. Res. Dev.*, 2003, **7**, 148-154.
- 21 T. V. Bukharkina and N. G. Digurov, *Org. Proc. Res. Dev.*, 2004, **8**, 320-329.
- 22 C. Guo, Q. Peng, Q. Liu and G. Jiang, *J. Mol. Catal. A*, 2003, **192**, 295-302.
- 23 S. Vetrivel and A. Pandurangan, *Appl. Catal. A*, 2004, **264**, 243-252; S. Vetrivel and A. Pandurangan, *Ind. Eng. Chem. Res.*, 2005, **44**, 692-701.
- 24 N. Novak Tušar, S. C. Laha, S. Cecowski, I. Arčon, V. Kaučič and R. Gläser, *Micropor. Mesopor. Mater.*, 2011, **146**, 166-171.
- 25 V. R. Choudhary, J. R. Indurkar, V. S. Narkhede and R. Jha, *J. Catal.*, 2004, **227**, 257-261; V. R. Choudhary, D. K. Dumbre, B. S. Uphade and V. S. Narkhede, *J. Mol. Catal. A*, 2004, **215**, 129-135.
- 26 S. Jana, Y. Kubota and T. Tatsumi, *J. Catal.*, 2007, **247**, 214-222.
- 27 A. Oussaid and A. Loupy, *J. Chem. Res.*, 1997, 342-343.
- 28 A. Shaabani, A. Bazgir, F. Teimouri and D. G. Lee, *Tetrahedron Lett.*, 2002, **43**, 5165-5167.
- 29 Y. Kuwahara, W. Kaburagi and T. Fujitani, *RSC Adv.*, 2014, **4**, 45848-45855.
- 30 K. Nagashima, T. Mitsudome, T. Mizugaki, K. Jitsukawa and K. Kaneda, *Green Chem.*, 2010, **12**, 2142-2144.
- 31 S. G. Stepanian, I. D. Reva, E. D. Radchenko and G. G. Sheina, *Vib. Spectrosc.*, 1996, **11**, 123-133.
- 32 M. Belli and A. Scafati, *Soild State Commun.*, 1980, **35**, 355.
- 33 N. M. D. Brown and J. B. Mcmonagle, *J. Chem. Soc. Faraday. Trans.*, 1984, **80**, 589-597.
- 34 F. Liu, W. Shan, Z. Lian, L. Xie, W. Yang and H. He, *Catal. Sci. Technol.*, 2013, **3**, 2699-2707.
- 35 K. Mori, H. Kakudo and H. Yamashita, *ACS Catal.*, 2014, **4**, 4129-4135.

View Article Online
DOI: 10.1039/C5CY01308A

Graphical Abstract



Mn(OH)_x supported on oxides *in-situ* transforms into monomeric Mn(III) species coordinated with PhCOO⁻ ligand, which efficiently oxidizes alkylaromatics with O₂.